

Electrical Performance from Bifacial Illumination International Space Station Photovoltaic Array

Ann M. Delleur* and Thomas W. Kerslake†

NASA John H. Glenn Research Center at Lewis Field, Cleveland, Ohio 44135

With the first U.S. photovoltaic array activated on the International Space Station in December 2000, on-orbit data can be compared to analytical predictions. Because of space station operational constraints, it is not always possible to point the front side of the arrays at the sun. Thus, in many cases, sunlight directly illuminates the backside of the array as well as albedo illumination on either the front or the back. During this time, appreciable power is produced because the solar cells are mounted on a thin, solar transparent substrate. It is important to present accurate predictions for both front and backside power generation for mission planning, certification of flight readiness, and on-orbit mission support. To provide a more detailed assessment of the power production capability, the authors developed a photovoltaic array electrical performance model applicable to generalized bifacial illumination conditions. We describe the space station photovoltaic array performance model and the methods used to reduce orbital performance data. Analyses were performed using SPACE, a NASA Glenn Research Center–developed computer code for the space station. Results showed an excellent comparison of on-orbit performance data and analytical results.

Introduction

THE International Space Station (ISS) is a complex spacecraft that will take several years to assemble in orbit. With the first U.S. photovoltaic array (PVA) launched, installed, and activated on flight 4A (early December 2000), the on-orbit data can now be compared to analytical predictions derived from the authors' previously published work on back-illuminated performance modeling¹ and albedo-enhanced performance modeling.^{2,3} A photograph of the U.S. PVAs (2B and 4B) on ISS is shown in Fig. 1.

Close-up photographs of the PVA wings after deployment were taken and are shown in Figs. 2 and 3. From a power perspective, it is best to point the front side of the arrays at the sun. However, several operational scenarios require that the arrays be held fixed, and thus the sun can directly illuminate the backside of the large U.S. solar arrays. For example, the U.S. ISS arrays are held stationary to minimize plume impingement from the space shuttle during docking and undocking as well as during shuttle wastewater dumps. In addition, many assembly and maintenance procedures also require that the arrays be held at fixed position for hours, which can significantly reduce power generation.

During the portions of the orbit when the backside is directly illuminated by the sun, appreciable power (about $\frac{1}{3}$ of front side power) is produced because the solar cells are mounted on a thin, solar transparent polymer substrate. Figure 3 shows the backside of PVA panels containing series-connected, 8×8 cm crystalline silicon solar cells with gridded back contacts and copper flat printed circuit interconnects.^{4–6}

It is important to present accurate power-generation predictions for mission planning, certification of flight readiness, and on-orbit mission support. Assessments of ISS electric power system performance have been performed by NASA Glenn Research Center using the code SPACE (System Power Analysis for Capability

Evaluation).^{7–9} SPACE has recently been validated with on-orbit data as described in a companion paper.¹⁰

To provide a more detailed assessment of the ISS power production capability, engineers at the NASA Glenn Research Center (GRC) collected and reduced ISS PVA orbital performance data during backside direct solar and Earth albedo illumination conditions. These data were compared with analytical predictions from the latest, bifacial PVA performance model, implemented in SPACE. This paper describes the methods used to process on-orbit data, the improved ISS PVA performance model, and the results from comparing SPACE analytical predictions with PVA orbital performance data.

PVA Telemetry

Orbits that had a significant portion of direct backside solar illumination with little to no shadowing were considered optimal for analysis. At moderate-to-high solar beta angles (the angle between the sun–Earth line and the orbit plane), significant shadowing of the arrays by the station structure or the shuttle occur. Because shadowing can reduce the number of active strings, recreating the available array current can be done with a shadowing factor, but for ease of analysis, orbits without shadowing were desired. Sun tracking the front side is the normal solar-array operation; thus, to have backside illumination with no shadowing, orbits with unusual array pointing at low solar beta angles were investigated. Once a possible time period was identified, the data were put through two tests to determine if there was indeed backside illumination as well as a sufficient time span of backside illumination to be useful for analysis. For the first test, the total array current I_{PVA} was plotted to determine if there were any periods where the current peak did not exceed 80A, the maximum current output for backside illumination.¹ If a candidate day passed the peak current test, then a second test on the data was needed to determine if the array were receiving significantly off-pointed, front-side illumination or direct solar backside illumination.

By converting the on-orbit telemetry for vehicle attitude and array orientation in to SPACE inputs, SPACE was run to generate station orientation and array view factors through the orbit to the sun, Earth, albedo, etc. If the array view factor showed direct solar illumination on the backside and the vehicle orientation through the orbit did not cause shadowing in the array, then the data were deemed acceptable for further study.

On 10 December 2001, during mission UF-1 the shuttle astronauts installed thermal blankets on both array gimbals during a 4-h

Received 7 October 2003; revision received 18 December 2003; accepted for publication 15 January 2004. This material is declared a work of the U.S. Government and is not subject to copyright protection in the United States. Copies of this paper may be made for personal or internal use, on condition that the copier pay the \$10.00 per-copy fee to the Copyright Clearance Center, Inc., 222 Rosewood Drive, Danvers, MA 01923; include the code 0022-4650/05 \$10.00 in correspondence with the CCC.

*Aerospace Engineer, Power and Propulsion Office, 21000 Brookpark Road; ann.delleur@grc.nasa.gov. Member AIAA.

†Aerospace Engineer, Power and Propulsion Office, 21000 Brookpark Road; Thomas.w.kerslake@grc.nasa.gov. Member AIAA.

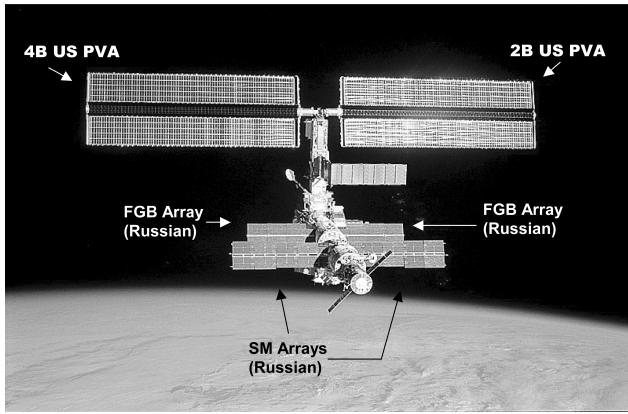


Fig. 1 ISS after shuttle separation, UF-1 Mission.



Fig. 2 ISS photovoltaic array wing (front side).

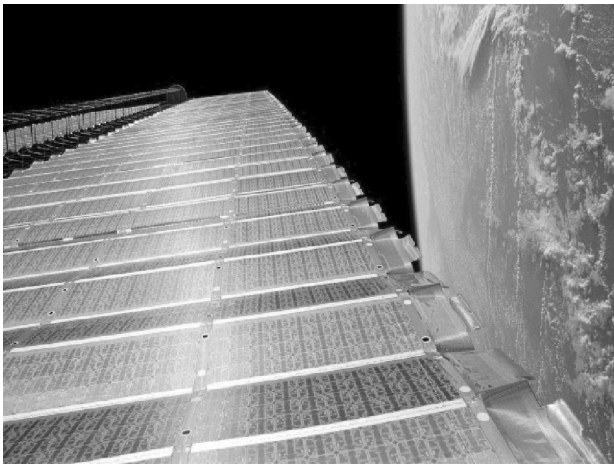


Fig. 3 ISS photovoltaic array wing (backside).

space walk. The arrays were parked 125 deg apart to allow astronaut access and optimize power generation. With the arrays fixed in this orientation, the starboard array, designated 2B, was solar illuminated on the front side for the first part of the orbit, then back illuminated. The 4B array, the port side array, observed the reverse, backside illumination first then front. The comparison of the predicted and measured PVA current production capability results for 2B were similar to those of 4B.

The second illustrated occurrence of backside illumination came from a crew sleep period on 2 February 2002, during an otherwise uneventful day.

The final occurrence of low solar beta backside illumination illustrated in this paper was taken from 12 April 2002, during the 8A mission with the shuttle docked, to install a major truss segment. The angle, at which the 4B array was parked, resulted in direct backside illumination during the first half of the orbit. Though the array was parked for many days, for purposes of illustration only one typical orbit is needed. Other relevant information for these mission days is summarized in Table 1.

PVA Data Processing

The PVA performance is measured by the sequential shunt unit (SSU) currents and voltage. When the array produces more power than is needed to meet the load current and battery charge current demand, excess array current is shunted in the SSU. A useful measure of PVA performance is the total available current production I_{PVA} given by

$$I_{PVA} = I_{SSU} + F_{corr} * I_{shunt} + I_{supply} \quad (1)$$

where I_{SSU} is the SSU output current, I_{shunt} is the SSU shunt current, I_{supply} is the SSU power supply current (0.4 amps), and F_{corr} is a correction factor (0.915) to estimate equivalent operating current based on the measured shunt current. F_{corr} accounts for 1) the shift from shunt current (near short-circuit current) to operating current (near peak power point current); 2) current-voltage (IV) operating point to accommodate voltage drops in the cell interconnects, power harness/cabling, and SSU shunt element; and 3) the shift in operating temperature ($\sim 5^\circ\text{C}$) between a shunted and operating solar-cell string. If necessary, a string shadowing correction factor can also be calculated using SSU shunt circuit control telemetry and calculated PVA shadow patterns. Shadowed PVA current output results are discussed elsewhere.¹¹ The measurement error is $+0\%/ -1\%$ and $+0\%/ -3\%$ for SSU output current and shunt current, respectively.

PVA Performance Model

Direct Illumination

The solar-cell IV curve during front or back illumination was modeled with cell current I as an exponential function of operating voltage V (Ref. 12):

$$I = I_{sc} - I_o * \{ \exp[q * (V - I * R_s) / \gamma * k * T] - 1 \} - V / R_{sh} \quad (2)$$

with γ as the curve-fitting parameter; I the cell current; k the Boltzmann constant; I_o the cell diode saturation current, $5.8\text{E}-09\text{ A}$; q the electron unit charge; R_s the cell series resistance; R_{sh} the cell shunt resistance; T the cell absolute temperature; and V the cell voltage.

The cell shunt resistance was assumed to be very large so that the V/R_{sh} term vanishes. The unknown terms of this equation, I_o , R_s , and γ , were determined based on the instantaneous values of cell front-side short-circuit current I_{sc} , open-circuit voltage V_{oc} , maximum-power-point current I_{mp} , and maximum-power-point voltage V_{mp} . For solar-illuminated front-side performance, instantaneous values were based on averaged, measured values obtained during front-side flash testing. These values were then corrected for orbital degradation factors, operating temperature, and solar pointing conditions.

For backside solar-illuminated performance, the cell IV values were originally based on backside flash test measurements over a range of incidence angles.¹ These back-illuminated cell IV values were normalized by normal-incidence front-side cell IV values. The normalized values were then multiplied by the instantaneous front-side cell IV values to obtain the instantaneous backside values.

In the current work, the backside performance model was improved. The backside (subscript b) V_{oc} values were used as measured, as a function of incidence angle θ . Other backside values were determined as follows:

$$I_{sc_b} = I_{sc} * I_r * \cos \theta \quad (3a)$$

$$I_{mp_b} = I_{mp} * I_r * \cos \theta \quad (3b)$$

$$V_{mp_b} = V_{mp} + R_s * (I_{sc} - I_{sc_b}) \quad (3c)$$

Table 1 On-orbit data

Day	Date	Stage	4B PVA	2B PVA	Solar β angle, deg	Calculated solar flux, W/m ²	Event
344	10 Dec. 01	UF-1 mission/shuttle docked	Parked	Parked	1.5	1414.2	EVA to install thermal blankets around the solar-array gimbals
33	02 Feb. 02	UF-1 stage/station alone	Parked	Sun tracking	24.2	1371.3	Crew presleep
102	12 April 02	8A mission/shuttle docked	Parked	Sun tracking	8.3	1364.6	Crew sleep

where I_r is the ratio of measured front side I_{sc} divided by the measured backside I_{sc} at normal incidence. These measurements include the effect of beginning-of-life solar absorption in the thin transparent polymer substrate on which the cells are mounted. Over time, the substrate transmittance decreases about one percentage point per year on orbit. This degradation effect is not accounted for in our present model and introduces about a 3% overprediction in I_r per year and a 3% overprediction in current produced from direct solar backside illumination. However, for sun tracking arrays, backside-albedo-generated current averages only about 5% of the front-side-current. Thus, the error introduced by ignoring substrate transmittance loss is only about 0.15% of the total bifacial array current for nominal sun tracking operations.

Albedo Illumination

Solar-cell front or back-albedo (subscript a) illuminated cell IV values were determined by scaling currents by the ratio of Earth albedo flux intensity to solar insolation flux and by adjusting voltages with current levels as follows:

$$I_{sc_a} = I_{sc}^* \text{albedo}/\text{insolation} \quad (4a)$$

$$V_{oc_a} = V_{oc}^* \ln(I_{sc_a}/I_o) / \ln(I_{sc}/I_o) \quad (4b)$$

$$V_{mp_a} = V_{mp} + R_s^*(I_{sc} - I_{sc_a}) \quad (4c)$$

$$I_{mp_a} = I_{mp}^* \text{albedo}/\text{insolation} + dI/dV|_{mp}^* (V_{mp_a} - V_{mp}) \quad (4d)$$

In these scaling relationships, based on Josephs,¹² the small performance impacts of albedo spectral and directional distributions were ignored. The small illumination contribution from ISS surface albedo was also ignored.

Bifacial Illumination

For generalized PVA illumination, there will be a direct solar component from the front or the back and albedo components on the PVA front and/or back. The solar-cell bifacial (subscript bf) IV values were calculated by superposing currents and scaling voltages with currents. Superposition was allowed as a result of the linear partial differential equations that describe the diffusion of electrons and holes in the solar cell junction.¹³ The resulting equation set, formulated for front-side direct solar illumination, was

$$I_{sc_{bf}} = I_{sc} + I_{sc_a} + I_{sc_{ab}} \quad (5a)$$

$$V_{oc_{bf}} = V_{oc}^* \ln(I_{sc_{bf}}/I_o) / \ln(I_{sc}/I_o) \quad (5b)$$

$$V_{mp_{bf}} = V_{mp} + R_s^*(I_{sc_{bf}} - I_{sc}) \quad (5c)$$

$$I_{mp_{bf}} = I_{mp}^* I_{sc_{bf}}/I_{sc} + dI/dV|_{mp}^* (V_{mp} - V_{mp_{bf}}) \quad (5d)$$

Once the bifacial solar-cell IV curve was obtained, the solar-cell string IV curve was calculated by summing the voltage contribution of the individual series-connected cells and subtracting the voltage drop in cell interconnects, string power harness/cabling, blocking diode, and SSU internal resistance. String current was iteratively determined such that cell voltage generation less line voltage loss

satisfied the SSU output voltage set point. In the presence of string shadowing, separate IV curves were calculated for shadowed and unshadowed string sections. In satisfying the SSU output voltage set point, three outcomes were possible for shadowed string current: 1) unshadowed cells provided all of the string current and voltage while shadowed cells were isolated with forward operating bypass diodes, 2) shadowed cells (with albedo illumination) current-limited all string solar cells and unshadowed and shadowed cells provided the string voltage, and 3) the string current was zero because of insufficient voltage generation to meet the SSU output set point voltage. Total PVA current capability was obtained by summing the current contribution of individual strings.

Based on analysis methods and data input uncertainties, the estimated uncertainty in calculated PVA current is $\pm 5\%$. Based on the short-term uncertainty in Earth albedo and infrared emission, the estimated uncertainty in short-term PVA current is $\pm 3\%$ for a sun tracking orbit. Therefore, the total root-sum-squared uncertainty in calculated PVA current is $\pm 6\%$.

PVA Performance Comparisons

PVA back-illuminated performance data can be obtained when the solar tracking beta gimbal is locked. The sun vector sweeps over a range of incident angles on the PVA front and back sides. This situation did occur on 10 December 2001 during extravehicular operations. The measured and calculated values of PVA current capability are shown in Fig. 4 for the orbital sun period of one such orbit. At the start of the sun period (16.1 h), the 4B PVA backside is nearly normal to the sun vector. By 16.5 h, the ISS has moved through the orbit to place the 4B PVA edge-on to the sun vector. Nearing the end of the sun period (16.85 h), the 4B PVA is now oriented with near normal solar pointing on the array front side.

The qualitative comparison between measured and calculated PVA currents through the orbit sun period is excellent. Quantitatively, the rms difference between measured and calculated values was 3.0A on the back and 4.4A on the front. This is equivalent to approximately 2% of PVA front side current capability or 4% of PVA backside current capability. Front-illuminated current data are smooth and in good agreement with calculated values. Minor discrepancies in backside calculated vs measured currents are discussed in the next section.

The 4B PVA was also locked for several orbits on 12 April 2002. Measured and calculated values of PVA current capability are shown in Fig. 5 for the sun period of one orbit.

An excellent qualitative comparison exists between measured and calculated PVA current values. The rms difference between measured and calculated values was 2.4A on the backside and 5.0A on the front side. Compared to data from 10 December 2001, these data are smoother during backside illumination (5.45–5.75 h), but show more variation during front-side illumination (5.75–6.40 h).

The last comparison of PVA current capability was for an orbit on 2 February 2002, with PVA 4B locked (Fig. 6). As in the preceding comparisons, the qualitative agreement between measured and calculated values over the orbit sun period was excellent. The rms difference was 3.3A on the backside and 4.4A on the front side. Both front-illuminated and back-illuminated current values exhibit occasional small ripples

Discussion

The preceding three data sets illustrate ISS PVA performance over a wide range of front-side and backside solar illumination angles.

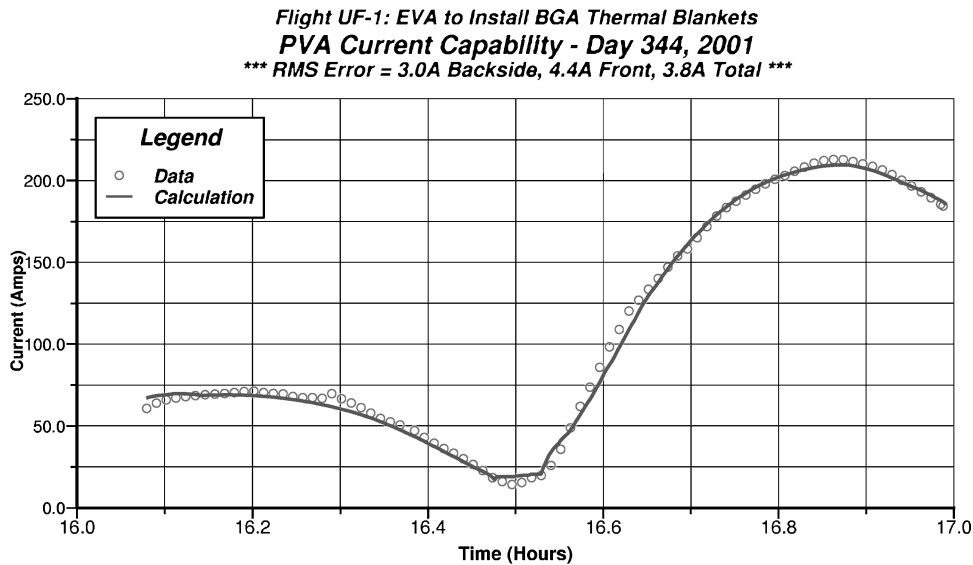


Fig. 4 Comparison of PVA current production capability (10 December 2001).

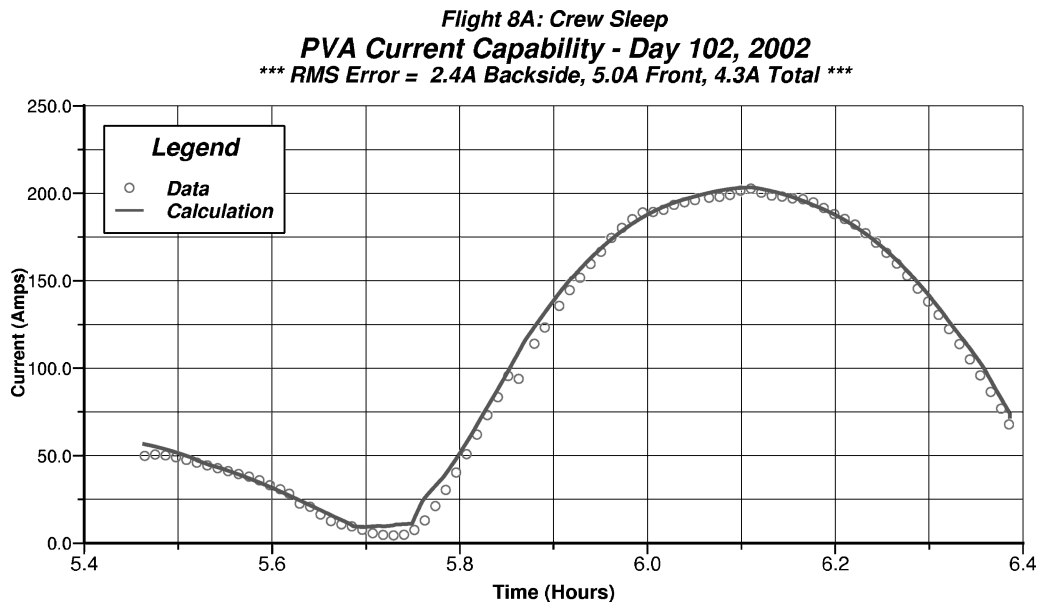


Fig. 5 Comparison of PVA current production capability (12 April 2002).

The excellent agreement between measured and calculated PVA current values demonstrates the bifacial performance model is sound. However, minor discrepancies in the comparison did exist for portions of the data. These differences are explained qualitatively in the paragraphs that follow.

In all three comparisons, current was overpredicted 10 to 15% at the start of the sun period. At this point in the orbit, the PVA operating temperature is approximately -80°C . At this temperature, the bandgap of crystalline solar cells increases, and the solar-cell spectral response (front and back sides) is diminished in the red and infrared part of the spectrum. During PVA back illumination, sunlight must pass through the polyimide substrate, which filters short wavelengths but allows longer wavelengths to pass. Thus, the red-dominated backside PVA current production is much more sensitive to the cold, post-eclipse operating temperatures than PVA front illuminated current production. In the computational model, solar-cell temperature coefficients are employed to account for temperature-dependent current-voltage performance. These coefficients were derived from front-illuminated cell flash test data and do not properly

account for the red-shifted, back-illuminated solar-cell performance temperature dependence. Thus, very cold (-80°C) back-illuminated PVA currents will be overpredicted. However, the lightweight PVA warms quickly and is at 0°C within ~ 3 min following orbit sunrise. Therefore, the error introduced in the total ampere-hours produced by the PVA over an orbit sun period is very small.

A second discrepancy was that minimum PVA currents were overpredicted by about 5 A during near edge-on solar illumination conditions for mission days on 10 December 2001 (3-min period of time at about 16.50 h in Fig. 4) and on 12 April 2002 (3-min period of time at about 5.75 h in Fig. 5). For these short periods, PVA current was generated exclusively by albedo illumination. The most likely explanation for this was that the attached space shuttle orbiter and the FGB and service module PVAs were blocking a portion of Earth albedo flux that illuminated the U.S. PVA front and back surfaces. This was determined by reviewing ISS flight attitude animations produced by SPACE. In SPACE, view factors to major ISS surfaces, including the FGB and service module arrays, were calculated. The sum of these view factors were used in the PVA thermal model as

Stage UF-1: Crew Pre-Sleep
PVA Current Capability - Day 033, 2002
 *** RMS Error = 3.3A Backside, 4.4A Front, 4.1A Total ***

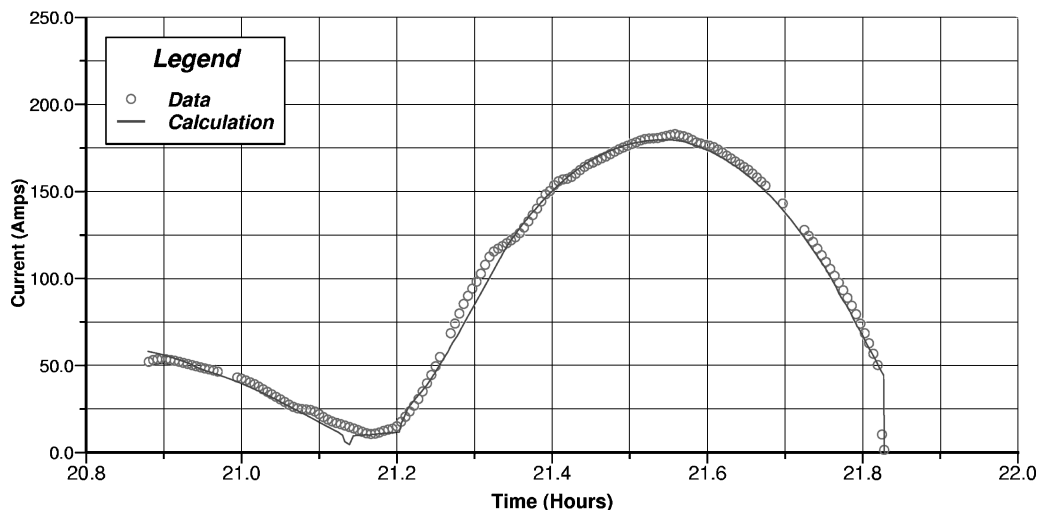


Fig. 6 Comparison of PVA current production capability (2 February 2002).

a reduction in radiation view factor to deep space. Reduction in Earth radiation, or Earth albedo fluxes, was not included in SPACE. As such, diminished Earth albedo fluxes from ISS surface blockage were not modeled and would lead to a small overestimation in PVA current. In contrast, PVA current nicely matched the data during near edge-on solar illumination on 2 February 2002 (time period near 21.15 h in Fig. 6). After reviewing the ISS flight attitude animation, it was clear that the view to Earth at this time was unobstructed by major ISS surfaces.

The last discrepancies were minor PVA current “ripples” observed for these mission days. Current ripples were characterized by the measured currents varying above and below the smooth predicted current profile over a several minute period of time. After reviewing the ISS attitude animations, it was clear these ripples coincided with special sun angles on the ISS and space shuttle orbiter, if attached. On 10 December 2001 at about 16.2–16.4 h (Fig. 4), the service module PVA albedo flux to the 4B PVA front side was maximized. Later in the same orbit, around 16.6–16.9 h, orbiter albedo to the 4B PVA backside was maximized followed by 4B PVA shadowing onto the orbiter (essentially eliminating orbiter albedo flux). The same orbiter albedo flux situation occurred late in the orbital sun period on 12 April 2002, at about 5.9–6.2 h (Fig. 5). Last, on 2 February 2002, at about 21.1 h (Fig. 6) the service module PVA albedo flux to the 4B PVA front side was maximized. Slightly later in the orbit, at about 21.3 h, the service module and FGB module PVA albedo fluxes were maximized to the 4B PVA backside. The small current dip at 21.7 h is caused by a conservative application of array pointing error used in SPACE. The pointing error is applied in the direction that results in minimum power, which can cause large differences between SPACE and on-orbit data at high off pointing angles.

The impact of these spacecraft-created albedo fluxes was to slightly increase measured PVA current output. Although the view factors to other ISS PVAs were calculated in SPACE, the view factor to the attached orbiter was not calculated. Because spacecraft view factors were not used to calculate spacecraft albedo fluxes onto the 4B PVA, calculated current output will be slightly underestimated for these brief periods of time when the ISS flight attitude and local sun angle conspire to maximize spacecraft albedo.

Summary

A computational model to predict ISS PVA electrical performance under generalized bifacial illumination conditions was developed. Telemetered PVA performance data for three different sample orbits over the period from December 2001 through April 2002 were ob-

tained and reduced. A comparison of these data with calculated PVA performance revealed an excellent qualitative agreement. The rms difference in measured and calculated PVA currents was well within the $\pm 6\%$ uncertainty in the PVA performance model. This indicated that the SPACE bifacial PVA performance model was sound. Minor discrepancies were noted in the comparison of calculated and telemetered PVA current data. The likely causes for these discrepancies were discussed.

The updates to this PVA performance model have increased its correlation with on-orbit data. With this more accurate modeling capability, improved power predictions that support on-orbit operations, certification for flight readiness, and mission planning can be made. To better predict aging of the arrays, the bifacial model will be updated to include substrate transmittance degradation and on-orbit hardware failures as they are identified. The bifacial performance code developed by GRC has not only been incorporated into SPACE but is also incorporated in software used by the NASA Johnson Space Center Mission Operations Directorate for day-to-day on-orbit ISS operations planning. Since the authors' first paper on this matter,¹ the space station program office has come to rely on the power produced from the PVA backside for on-orbit operations and planning.

Acknowledgments

The authors thank Jeffrey S. Hojnik for his help with code development; Anthony Jannette for maintaining the on-orbit operations summary; all of the other members of the International Space Station electric power system analysis team at NASA Glenn Research Center for their assistance; and Lou Ignaczak, Dave McKissock, and Bruce Manners for their reviews.

References

- Delleur, A. M., Kerslake, T. W., and Scheiman, D. A., “Analysis of Direct Solar Illumination on the Backside of Space Station Solar Cells,” *Proceedings of the 34th Intersociety Energy Conversion Engineering Conference*, Society of Automotive Engineers, Warrendale, PA, 1999.
- Kerslake, T. W., and Hoffman, D. J., “Mir Cooperative Solar Array Flight Performance Data and Computational Analysis,” NASA TM-1997-107502, July 1997.
- Kerslake, T. W., and Hoffman, D. J., “Performance of the Mir Cooperative Solar Array After 2.5 Years in Orbit,” NASA TM-1999-209287, July 1999.
- Vogt, S. T., and Proeschel, R. A., “Space Station Photovoltaic Power Module Design,” *Proceedings of the 23rd Intersociety Energy Conversion Engineering Conference*, Vol. 3, American Society of Mechanical Engineers, New York, 1988, pp. 567–572.

⁵Hashmi, A. T., "Space Station Freedom Solar Array Development Testing," *Proceedings of the 28th Intersociety Energy Conversion Engineering Conference*, Vol. 1, American Chemical Society, Washington, DC, 1993, pp. 365–370.

⁶Lillington, D. R., Kukulka, J. R., Nasib, A. V., Sater, B. L., and Sanchez, J., "Optimization of Silicon 8 cm \times 8 cm Wrap Through Space Station Cells for 'On Orbit' Operation," *Proceedings of the 20th Institute of Electrical and Electronic Engineering Photovoltaics Specialist Conference*, Vol. 2, Inst. of Electrical and Electronics Engineers, New York, 1988, pp. 934–939.

⁷Hojnicki, J. S., Green, R. D., Kerslake, T. W., McKissock, D. B., and Trudell, J. J., "Space Station Freedom Electrical Performance Model," *Proceedings of the 28th Intersociety Energy Conversion Engineering Conference*, Vol. 2, American Chemical Society, Washington, DC, 1993, pp. 869–874.

⁸Fincannon, J., Delleur, A., Green, R. D., and Hojnicki, J. S., "Load-Following Power Timeline Analyses for the International Space Station," *Proceedings of the 31st Intersociety Energy Conversion Engineering Conference*, Vol. 1, edited by P. R. K. Chetty, W. D. Jackson, and E. B. Dicks, Inst. of Electrical and Electronics Engineers, Piscataway, NJ, 1996, pp. 185–190.

⁹Kerslake, T. W., Hojnicki, J. S., Green, R. D., and Follo, J. C., "System Performance Predictions For Space Station Freedom's Electrical Power Sys-

tem," *Proceedings of the 28th Intersociety Energy Conversion Engineering Conference*, Vol. 2, American Chemical Society, Washington, DC, 1993, pp. 863–868.

¹⁰Jannette, A. G., Hojnicki, J. S., McKissock, D. B., Fincannon, J., Kerslake, T. W., and Rodriguez, C. D., "Validation of International Space Station Electrical Performance Model via On-Orbit Telemetry," *Proceedings of the 37th Intersociety Energy Conversion Engineering Conference*, Inst. of Electrical and Electronics Engineers, Piscataway, NJ, 2002.

¹¹Fincannon, H., and James, "Comparison of ISS Power System Telemetry with Analytically Derived Data for Shadowed Cases," *Proceedings of the 37th Intersociety Energy Conversion Engineering Conference*, Inst. of Electrical and Electronics Engineers, Piscataway, NJ, 2002.

¹²Josephs, R. H., "Solar Cell Array Design Handbook," NASA CR-149364, Oct. 1976.

¹³Bordina, N. M., Zayavlin, V. R., Kagan, M. B., and Letin, V. A., "Solar Batteries with Bifacial Sensitivity," *Geliotekhnika*, Vol. 28, No. 1, 1992, pp. 39–47.

A. Ketsdever
Associate Editor